Surface & Coatings Technology 476 (2024) 130197

Contents lists available at ScienceDirect

Surface & Coatings Technology

journal homepage: www.elsevier.com/locate/surfcoat

Influence of fitting algorithms on thickness determination during monitoring of optical coatings

Thomas Melzig [a,*], Tatiana Amochkina [b], Stefan Bruns [a], Philipp Farr [a], Jörg Terhürne [c], Michael Trubetskov [b,d], Michael Vergöhl [a]

[a] Fraunhofer Institute for Surface Engineering and Thin Films IST, Optical Systems and Applications, Riedenkamp 2, 38108 Braunschweig, Germany
[b] OTF Studio GmbH, Watzmannring 71, 85748 Garching, Germany
[c] Bte Bedampfungstechnik GmbH, Am Ganzacker 2, 56479 Elsoff, Germany
[d] Max-Planck Institute of Quantum Optics, Hans-Kopfermann Str. 1, 85748 Garching, Germany

ARTICLE INFO

Keywords:
Broadband optical monitoring
Transmittance
Thickness measurement
Process control
Magnetron sputtering
Optical coating

ABSTRACT

The monitoring of thickness evolution during the deposition of optical interference coatings is widely performed by transmittance measurements and continuous comparison with theoretical models. The fitted thickness of the actual layer is influenced by the quality of the signal. Effects from light path, substrate and spectrometers result in deviations because these are often not part of the models. We show an implementation of these unmodeled effects in the fitting algorithms. The outcome of different configurations while coating the same optical filter design is compared. Additionally, the time consumption of these strategies is investigated to verify their suitability for production.

1. Introduction

Broadband monitoring is gaining more and more popularity in the state-of-the-art thin-film production (see for example, [2–5,7]. Tremendous progress in the development of numerical tools as well as technical instrumentation has been achieved by several leading research groups and companies. One of the most challenges in this area is monitoring of antireflection coatings since they contain typically thin layers (<10 nm). Very often, one of the thin layers is the first layer. It means that there is only a small signal change in the transmittance measurement. This makes it difficult to determine the exact thickness of this layer. Nevertheless, this layer is important for antireflection performance of the coating. To solve this issue, it is common to fit the thickness of previous layers again together with the measurements of the following layers [1–4].

In this work we used the Modular Optical Monitoring Control Application (MOCCA^{+}®) developed by Fraunhofer IST [5] together with the software tool taReo developed by OTF Studio to successfully show the production of these kind of antireflective coatings on the FHR. Star.600-EOSS® (Enhanced Optical Sputtering System) at Bte Bedampfungstechnik [6–10]. We present an approach to compensate errors in the measurement signal and a comparison of different numerical data-processing algorithms also referred as fitting strategies.

In chapter 2 we describe the experimental setup consisting of the coating machine and the two software tools. Furthermore, the different fitting strategies and compensation models are explained. The last chapter gives a discussion of the time consumption and a comparison of selected runs from production using the adapted models.

2. Experimental setup

2.1. Coating system

Coating experiments were conducted at Bte using a FHR.Star.600-EOSS® (Enhanced Optical Sputtering System). The system has two magazines with 15 places respectively for substrates up to (330 × 280) mm^2 and an automatic handling system for 24/7 production. The main coating chamber is under permanent vacuum and holds a turntable with 12 places for substrates and three dual rotatable magnetron sputter stations in sputter up configuration (Fig. 1). Two stations were equipped with NbOx targets driven by a CARS process (Compound assisted reactive sputtering) and silicon targets driven by a MetaMode™ process [9]. The sputter generators work with mid-frequency. Sputtering takes place in pure Ar atmosphere. Oxidation of the sputtered material takes place

* Corresponding author.
E-mail address: thomas.melzig@ist.fraunhofer.de (T. Melzig).

https://doi.org/10.1016/j.surfcoat.2023.130197
Received 1 September 2023; Received in revised form 27 October 2023; Accepted 11 November 2023
Available online 17 November 2023

in an additional radio-frequency driven plasma source. The turntable has a speed of up to 250 rounds per minute (rpm), while 125 rpm were used in the present work. Thus, only thin layers with <0.1 nm are deposited at each rotation to ensure that the oxidation leads to fully stoichiometric films.

2.2. MOCCA$^+$® and light path-

The EOSS® coating system at Bte is driven by MOCCA$^+$® (Modular Optical Coating Control Application) [6–10]. The software allows full control of all relevant system parameters like sputter sources, gas flows, shutters and handling. Layer stacks from optical design software are connected to individual layer recipes that are stored in a database. Broadband transmittance measurements are used to monitor the layer thickness during deposition of the actual layer and stop the coating at desired thickness [5,11].

A halogen lamp is used for illumination through a multimode fiber and a collimator outside the machine. The light passes the quartz entrance window, then the turntable with the coated sample on the substrate carrier and afterwards the exit window. After this air-vacuum-air part it is coupled into a multicore fiber by a collimator again. One part of the fiber bundle is attached to the VIS spectrometer and one part is attached to the NIR spectrometer (Fig 2). The linear silicon sensor for UV-VIS has 1024 pixels and the linear InGaAs sensor for NIR has 512 pixels. Both sensors have a low signal-to-noise ratio (SNR) at fast integration times of 3–4 ms that are required due to the high turntable rotation speed. Dark, reference and sample measurements are recorded at each rotation. This means a full spectrum is available every 240 ms at 250 rpm or, in the present case, every 480 ms at 125 rpm. The used transmittance band ranges from 380 to 1650 nm. Typically, both spectrometers with a combined wavelength range of 400 to 1600 nm are used for optical monitoring. In some cases, depending on the spectral properties of the coating, the wavelength range is reduced.

2.3. taReo numerical algorithms and software library

taReo is a powerful software tool developed to support the production of multilayer optical coatings in deposition machines equipped with devices capable of acquiring in situ measurements during the coating process. One implementation of such devices is broadband optical monitoring, which involves measuring the transmittance or reflectance of a test glass sample placed alongside the substrates in the deposition chamber. The device can record in situ data flow: measurement spectra after the deposition of each coating layer, as well as measurement scans taken in very short time intervals during the deposition of each layer.

An optical coating being produced can be represented as a model multilayer described by its layer thicknesses and optical constants of thin-film materials and a substrate. Model data is transmittance or reflectance of the model multilayer. taReo is based on numerical algorithms, minimizing discrepancies between experimental and model data with respect to layer thicknesses. Generally, a discrepancy function can be represented as:

$$DF = \left(\frac{1}{L} \sum_{j=1}^{L} \left[T(X;\lambda_j) - \widehat{T}_{exp}(\lambda_j) \right]^2 \right)^{1/2} \quad (1)$$

where X is the vector of model parameters, T is model spectral characteristic, and T_{exp} is experimental spectral characteristic measured at the wavelength grid $\{\lambda_j\}, j = 1,..,L$ The representation of the vector X is dependent on the algorithm chosen for data processing described in detail in chapter 2.5.

Also, based on the discrepancy function minimization, estimation of the deposition rate can be performed and the time remaining until the end of the layer deposition can be accurately predicted.

Re-optimization of the remaining layers can be performed if necessary. In this case, in Eq. (1), the vector X represents thicknesses of the remaining layers. Experimental data points in Eq. (1) are replaced by the desired coating specifications.

From the software point of view, taReo can communicate with external programs using either direct DLL calls or COM Automation technologies. taReo uses highly effective computational algorithms, harnessing the modern architecture of processors and enabling parallel calculations on systems with multi-core processors.

Computations are being performed very quickly even dealing with many dozens of layers. Characterization and re-optimization are done in real-time, without interruption of the deposition process.

2.4. MOCCA$^+$® and taReo

MOCCA$^+$® is responsible for the process configuration, measurements and communicates with taReo via a DLL interface. The measured transmittance spectra recorded either after or during the deposition of

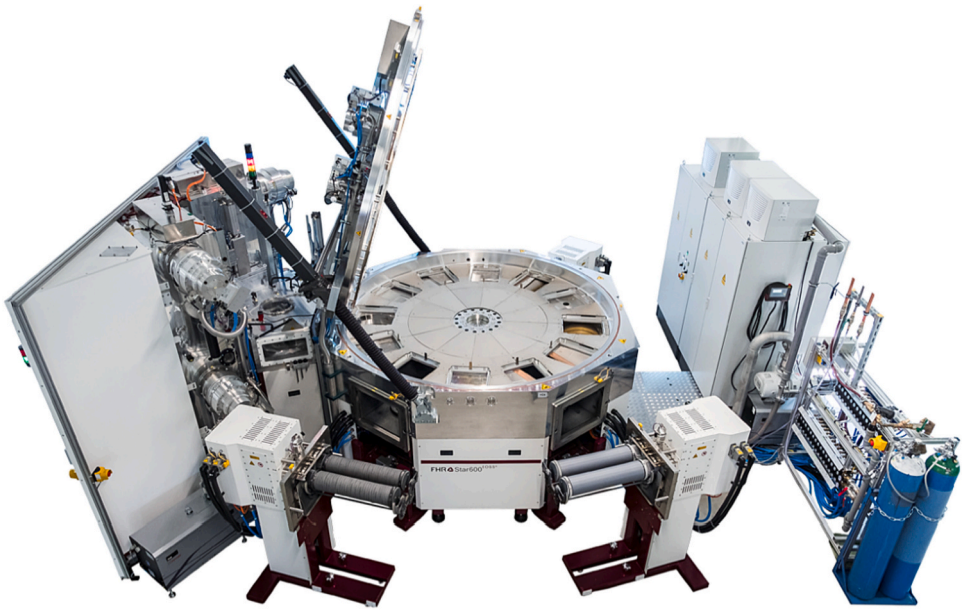

Fig. 1. EOSS at Bte.

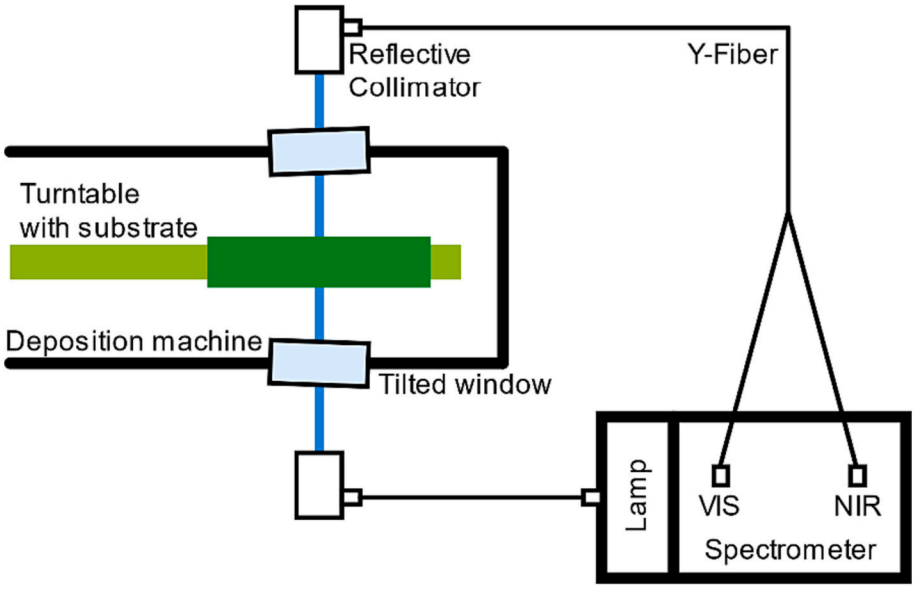

Fig. 2. MOCCA+® light path.

each layer are sent to taReo, and the respective numerical algorithms (fitting strategies) are called. These fitting strategies are described in chapter 2.5 and illustrated in Fig. 3. In this study, taReo performs characterization either with the help of the sequential or by using the triangular algorithms. taReo determines thicknesses of the previously deposited layers (in the case of triangular algorithms) and the thickness of the current layer and estimates the time remaining until the end of the layer deposition. taReo sends the results (layer thicknesses, termination points) back to MOCCA^{+}® that makes final decision on layer termination. Then MOCCA^{+}® terminates the layer deposition.

2.5. Fitting strategies

In our work we used three different fitting strategies, "pre-calculation", "sequential" and "triangular". All of them use the design of the layer stack and the dispersion data of the substrate and the coating materials as inputs. Fitting strategies "pre-calculation" and "sequential" are used alternatively during deposition while "triangular" is usually used after every layer. In this work we use only "pre-calculation" fit to terminate layers in combination with "triangular" fit.

The fitted thicknesses may deviate from theoretical thicknesses not only due to measurement error like noise or detector step but also to a lack of accuracy in dispersion data.

2.5.1. The pre-calculation strategy

This strategy, illustrated in Fig. 3a, is implemented in the MOCCA^{+}® software and calculates the spectral transmittance of a given layer based on the aforementioned inputs and the fitted thicknesses of all previous layers. These calculations are done once before the start of the i-th layer. The n pre-calculated spectra differ only in the thicknesses $d_{i,1}$ to $d_{i,n}$ of the current layer, typically in steps of 0.1 nm. During the coating of this layer the measured transmittance spectra are then compared with the pre-calculated ones to determine the current thickness and are also used for the endpoint detection. The closeness is estimated based on the minimization of the discrepancy function:

$$DF^{precalc}(i) = min_{k=1,\ldots,n}\left[\left(\frac{1}{L}\sum_{j=1}^{L}\left[T\left(d_1^f,\ldots,d_{i-1}^f,d_{i,k};\lambda_j\right)-\widehat{T}_{exp,i}\left(\lambda_j\right)\right]^2\right)^{\frac{1}{2}}\right] \quad (2)$$

where $i = 1,\ldots,m$ and m is the number of design layers, $d_1^f,\ldots,d_{i-1}^f$ are fitted layer thicknesses; d_i is the thickness of the current i-th layer; $T_{exp,i}$ is the experimental transmittance recorded after the deposition of i-th layer. The back side compensation model (see chapter 2.6) is currently only implemented for the pre-calculation strategy.

2.5.2. The sequential strategy

This strategy, illustrated in Fig. 3b, is implemented in taReo and also uses the fitted thicknesses of all previous layers as an input. The difference to the pre-calculation strategy is that the thickness of the current i-th layer is fitted with an optimization loop based on the minimization of the discrepancy function:

$$DF^{seq}(i) = \left(\frac{1}{L}\sum_{j=1}^{L}\left[T\left(d_1^f,\ldots,d_{i-1}^f,d_i;\lambda_j\right)-\widehat{T}_{exp,i}\left(\lambda_j\right)\right]^2\right)^{1/2},\quad i=1,\ldots,m \quad (3)$$

In Fig. 3b, fitted thicknesses of layers 1–4 are schematically shown, layer number 5 is being deposited and d_6^t, d_7^t, d_8^t are theoretical thicknesses of the remaining layers.

2.5.3. The triangular strategy

The triangular strategy, illustrated in Fig. 3c, is also implemented in taReo but uses the transmittance measurements recorded at the end of all previous layers instead of their thicknesses. Then, together with the transmittance spectrum during the layer coating, the thicknesses of all layers of the design including the current one are fitted with an optimization loop based on the minimization of the discrepancy function:

$$DF^{triang}(i) = \left(\frac{1}{i}\sum_{k=1}^{i}\frac{1}{L}\sum_{j=1}^{L}\left[T\left(d_1^f,\ldots,d_{i-1}^f,d_i;\lambda_j\right)-\widehat{T}_{exp,i}\left(\lambda_j\right)\right]^2\right)^{\frac{1}{2}} \quad (4)$$

In Fig. 3c, it is illustrated that during the deposition of the 5th layer, layer thicknesses of the layers 1–4 as well as the thickness of the current 5th layer are being fitted. For all runs presented in this paper, the maximum permitted thickness deviation was set to 5 %.

2.6. Compensation models

In this paper we use two different models to compensate for all unmodeled effects in the transmittance spectra. The back side model is explained in detail in a previous paper [5]. The basic idea is to include all deviations of the measurement from the theoretical substrate

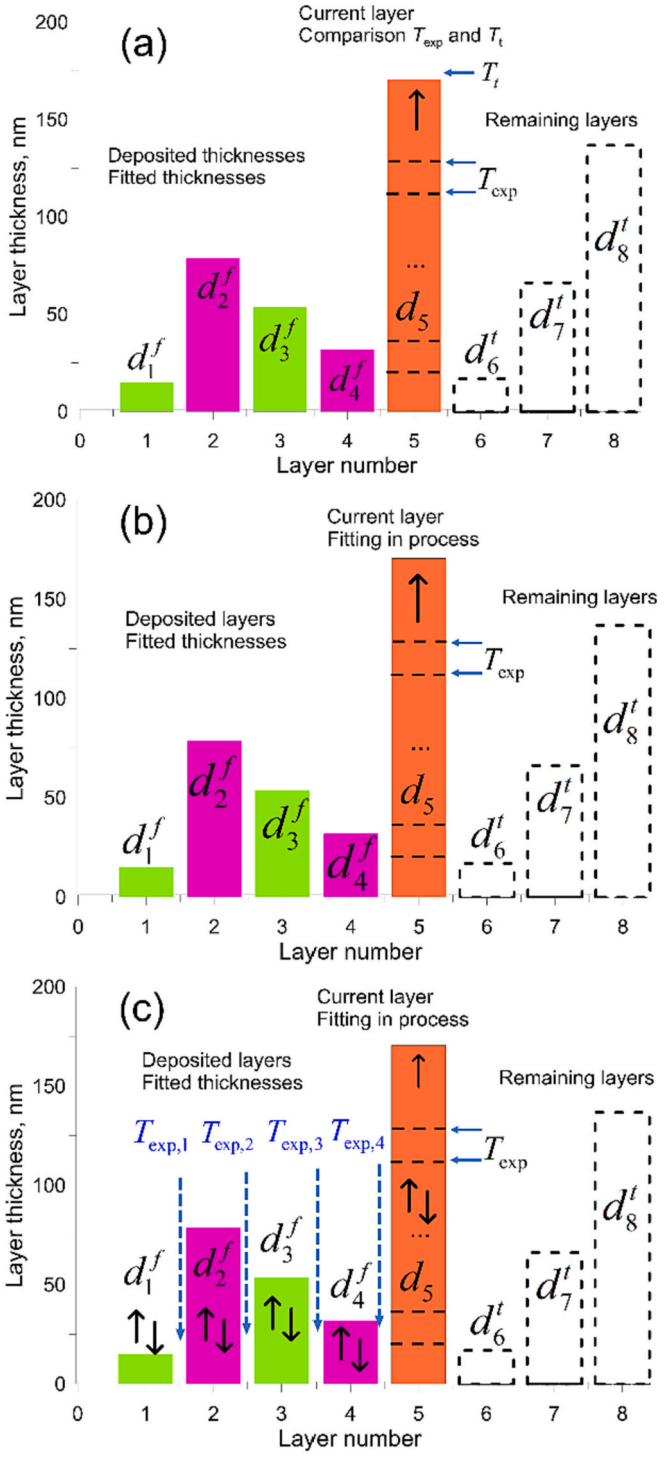

Fig. 3. Schematic illustration of three fitting strategies: pre-calculation (a), sequential algorithm (b), and triangular algorithm (c).

transmittance into the calculation of the transmittance of the coating itself as virtual backside coating. Therefore, the used thin film calculation library has to offer this compensation model as an option, which is the case for MOCCA^{+}® but not for other libraries like taReo or OptiLayer/OptiReOpt.

The factor model on the other side calibrates a transmittance measurement of an uncoated substrate, the so-called pre-measurement $T_{pm}(\lambda)$, to its theoretical transmittance $T_{sub}(\lambda)$. These spectral calibration factors will be applied to all further transmittance measurements $T_{meas}(\lambda)$ in order to get a compensated transmittance:

$$T_{comp}(\lambda) = T_{meas}(\lambda)\frac{T_{sub}(\lambda)}{T_{pm}(\lambda)} \tag{5}$$

The compensated transmittance is then used for the optical monitoring and fed into the thin film calculation library, which is taReo in this paper.

3. Results and discussion

3.1. Time consumption of fitting algorithms

An important point of the decision for a fitting algorithm is its time consumption. In the given setup the turntable rotates with a speed of 125 rpm which means one measurement every 480 ms. In the best case the algorithms are fast enough to process every measured spectrum. Obviously, in the triangular algorithm, the calculation time is growing with the number of layers, i.e., the number of optimization parameters increases. With a large number of layers (about 100), the calculation time can exceed the time between two measurements. This is the reason, that in some situations, either every nth measurement can be used or another algorithm should be chosen (for example, a hybrid triangular algorithm where several last layers are being fitted at each step).

Fig. 4 shows the averaged fitting times during the individual layers in comparison of the pre-calculation and the sequential strategy. The experimental results of different coating designs with up to 32 layers are plotted. The specific times may be influenced by the material and the thickness of the layer, but the overall slope is independent of the design type and depends only on the layer number.

The times for the pre-calculation strategy are constant over the layer number and only fluctuate around 5–6 ms. The reason for this is that most of the calculations are made before the layer starts. The sequential strategy shows also constant and even lower fitting times. This is achieved with the help of a highly optimized mathematical core.

In Fig. 5 we compare the time consumption of the triangular strategy for multiple runs of the same design with different spectral bands active. If only the VIS band is active, less time is needed for the fit because the number of spectral points is lower than for VIS and NIR combined.

The used time of about 150 ms for the fit of 14 layers with the triangular strategy is much higher than the 10 ms for the sequential strategy and the same number of layers. These differences are expected since the number of parameters for the triangular fit are proportional to the layer number.

3.2. Influence of unmodeled effects in the transmittance spectrum on the fitting algorithms

Fig. 6 shows the influence of different compensation models on the fit results. The compensation is necessary because there are multiple unmodeled effects in the transmittance spectrum [12–14]. The effect at 950 nm, the so-called detector step, comes from the usage of two detectors, one for the VIS and the other for the NIR part of the spectrum (see Chapter 2.2). It varies with changes in the optical path when the process chamber is opened for cleaning or other services. In a production environment this happens roughly once a month. Minimization of the effect by manual recalibration of the optical path is possible but laborious. At 1400 nm an absorption band related to water in the substrate is located [15].

The three plots on the left show the measured transmittance signal (red curves) of the uncoated monitor substrate, the “pre-measurement”, together with the corresponding model (blue curves). These signals are recorded with (6c) and without averaging (6a and 6b), which explains the different noise levels. In (6a) and (6c) the blue curve shows the theoretical transmittance of an uncoated Borofloat monitor substrate. (6b) uses the back side model for compensation and shows the calculated result as the blue curve. For the factor model in (6c) the red and the

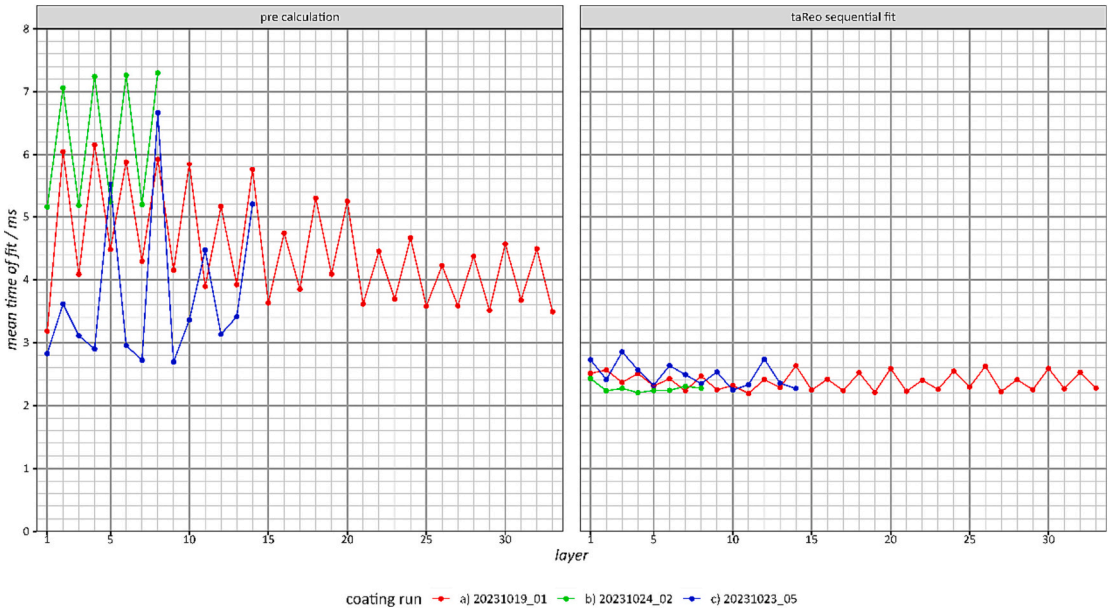

Fig. 4. Fit duration throughout coating of the layers for different designs shown for pre-calculation and taReo sequential fit algorithms.

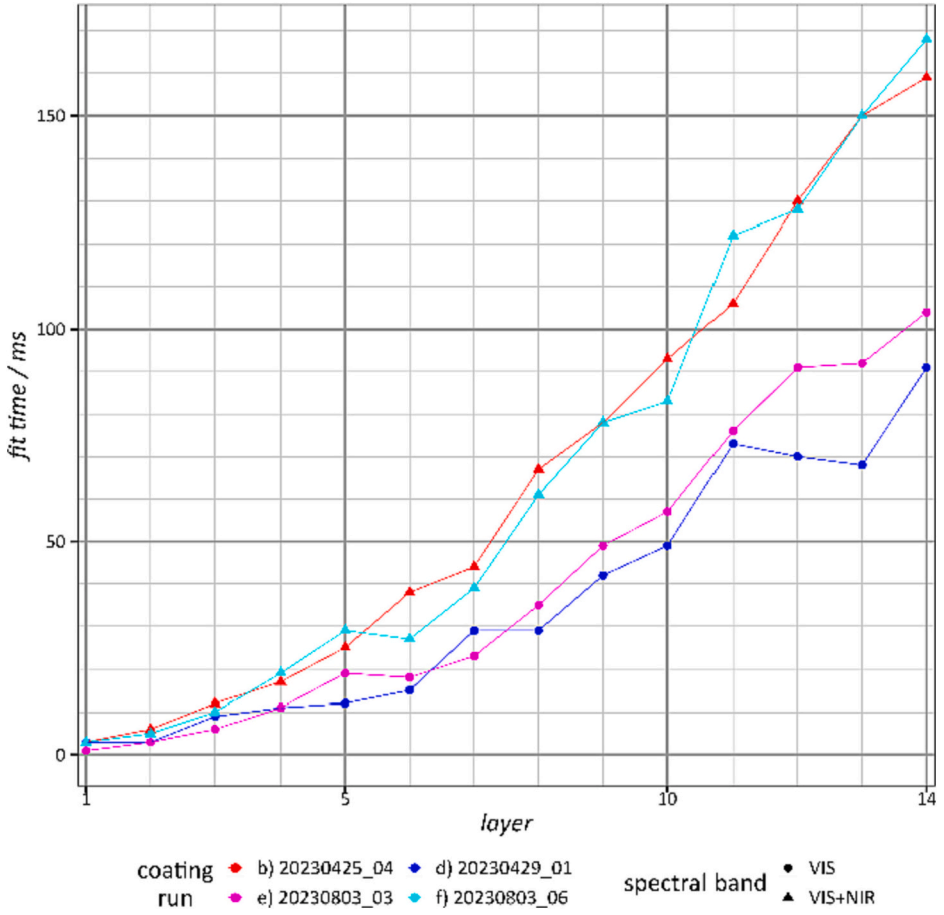

Fig. 5. Time consumption for triangular fit at the end of each layer in different configurations.

blue curves were used to calculate the spectral calibration factors. Therefore, the value of the discrepancy function is zero.

The three plots on the right show the transmittance signal after the deposition of a quarter wave layer of niobia. Without compensation (6d) the fit curve does not show a good agreement with the measurement. However, the value of the discrepancy function is not comparable with the ones of (6e) and (6f) because the unmodeled effect at 1400 nm was cut out.

For the VIS part of the spectrum the fitted transmittance is lower than the measurement, while for the NIR part it is higher. In case of

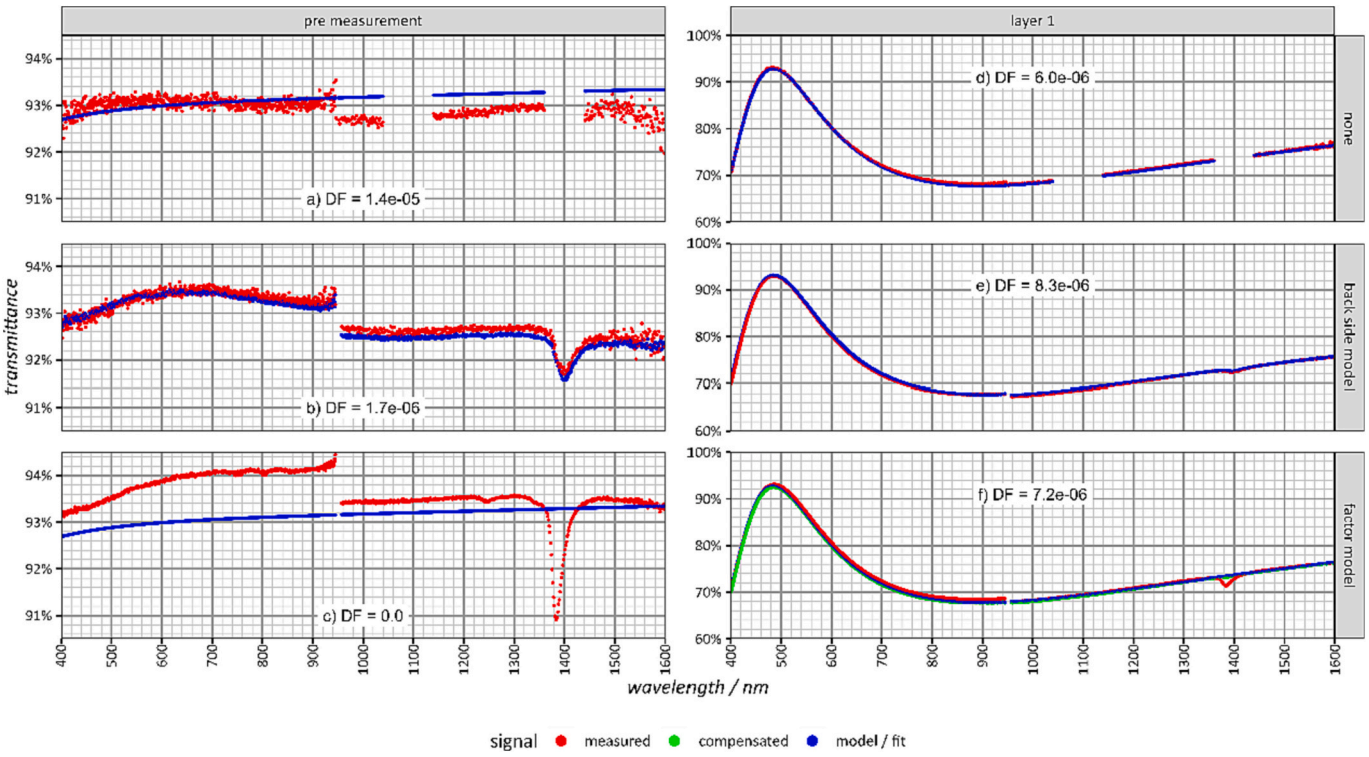

Fig. 6. Pre- and coating measurements are compared with its fits for different compensation models.

compensation with the back side model (6e), the agreement is better. For the factor model (6f), the compensated measurement curve (green) is additionally plotted. It also has a good agreement with the fit.

3.3. Determination of layer thickness

For the evaluation of different test conditions, a 14-layer AR coating on substrate Schott Borofloat 33 was used. The AR reflectance was specified to be below 1.5 % in the wavelength range from 430 nm to 900 nm and an angle of incidence (AOI) of 45° for the average of s- and p-polarized light (average polarized). In Table 1 the coating design is shown together with the discrepancy function value DF for wavelength 430 nm to 900 nm and the thickness deviations of run a), c) to e). Fig. 7 shows the design and ex situ reflectance measurements of five runs under different test conditions. The design is quite sensitive to deviations in the layer thickness. Run 7a used transmittance measurements from both spectrometers, VIS and NIR, with the back side model applied to the pre-calculation fit but not to the triangular fit. Run 7b also used both spectral bands, but only the pre-calculation with back side model applied. Run 7c then used only VIS band with the back side model

Table 1
Coating design of the 14-layer AR including absolute thickness deviations for all applicable runs.

Index	a)	c)	d)	e)
Run	20230425_04	20230429_01	20230803_03	20230803_06
Spectral band	VIS + NIR	VIS	VIS	VIS + NIR
Compensation model	back side model		factor model	
strategy	pre-calculation with triangular fit			
DF (430 nm to 900 nm)	0.361108	0.25644	0.284272	0.253553

Layer	Material	Theoretical thickness/nm	Deviations of fitted from theoretical thicknesses after layer 14			
			/nm	/nm	/nm	/nm
1	Nb2O5	9.723	−0.486	−0.448	0.257	−0.037
2	SiO2	55.9	−0.831	2.795	0.323	0.253
3	Nb2O5	28.102	0.16	−0.52	0.123	0.008
4	SiO2	16.378	0.819	−0.819	0.735	−0.819
5	Nb2O5	110.064	−3.76	−0.012	−1.082	0.294
6	SiO2	31.696	1.145	1.585	1.585	1.585
7	Nb2O5	18.534	−0.172	−0.505	−0.845	−0.729
8	SiO2	156.882	−0.435	−1.095	−0.96	−1.651
9	Nb2O5	12.056	−0.509	−0.432	−0.235	−0.333
10	SiO2	44.316	1.612	2.216	2.216	2.216
11	Nb2O5	78.814	0.552	0.082	−0.111	0.061
12	SiO2	6.013	0.301	0.301	−0.128	−0.301
13	Nb2O5	43.657	−0.19	−0.101	−0.251	0.011
14	SiO2	110.426	−1.687	−0.634	−0.079	−0.279

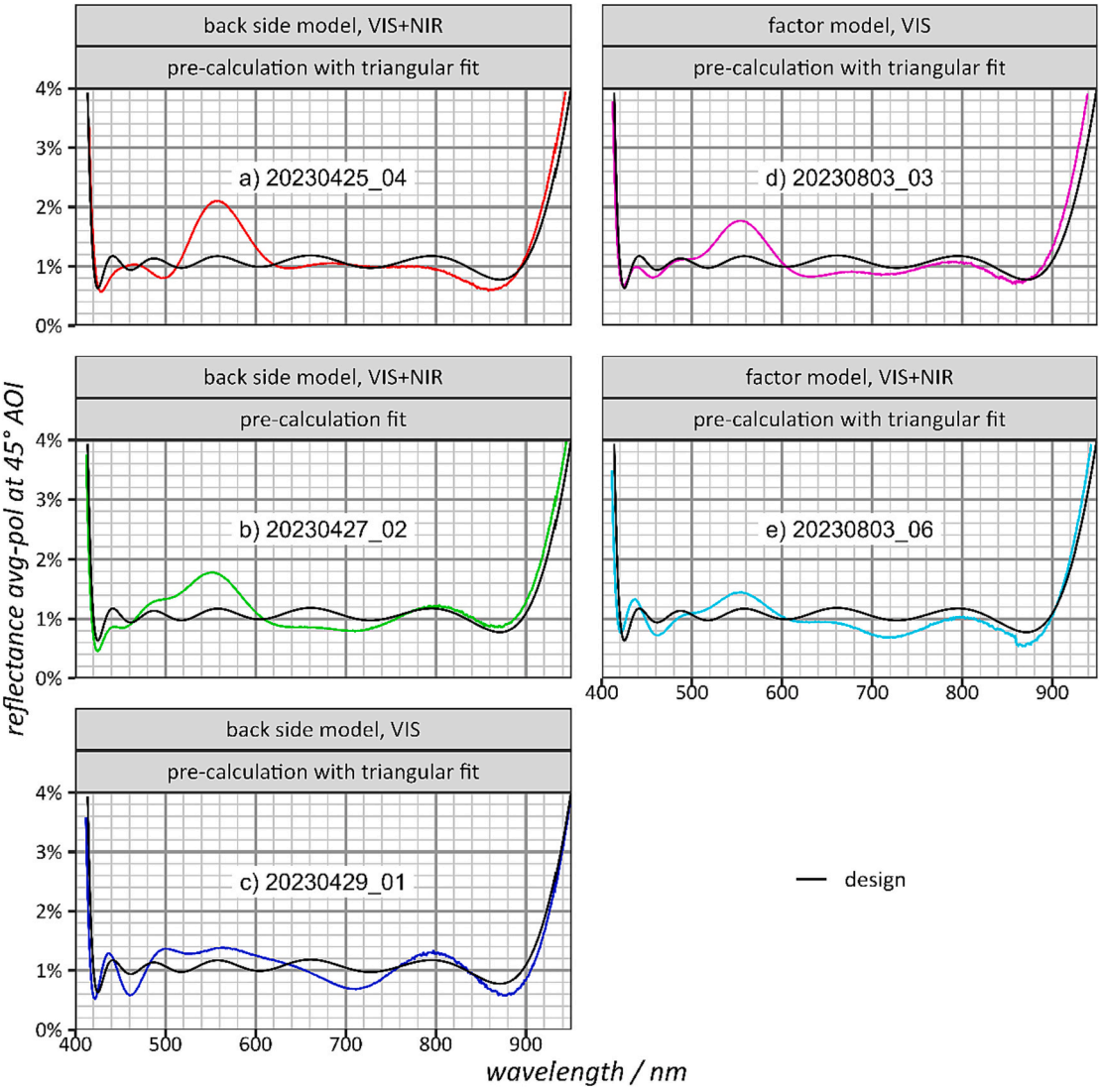

Fig. 7. Experimental results of a 14-layer AR coating for different combinations used spectral bands, compensation models and fitting strategies.

applied to the pre-calculation fit but not to the triangular fit. Run 7d also used only the VIS band but now the factor model was applied to the pre-calculation as well as to the triangular fit. Run 7e again used both bands and the factor model applied to both fitting algorithms pre-calculation and triangular. Runs 7c and 7e yield the best results while run 7a the worst. In run a) the VIS and NIR spectra were used in the triangular fit without a compensation model. Therefore, especially the detector step had a significant effect on the fit. In run c) only the VIS spectrum was used and in run e) the factor model was applied to VIS and NIR spectra.

In Fig. 8 the relative deviations of fitted thicknesses from design thicknesses are shown for layer 1 to 14 for the triangular fit algorithm. Since the thickness of a layer *n* is first fitted after it is finished but then refitted after all following layers, the fitted thicknesses evolve throughout the coating run. The cause for fitted thicknesses deviating from design thicknesses could be traced back to the use of spectral bands, compensation models and fitting strategies but also to thickness deviations of other layers. Nevertheless, thickness deviations of run 8a, the red curve and the worst result, show the greatest deviations of all, especially layer 1 and 5. Comparing the best results, run 8c, the blue curve, and run 8e, the cyan curve, 8e shows over all smaller deviations than 8c Layer 4 shows great deviations for all test conditions probably because the measured transmittance changes very little throughout depositing this thin layer of low-refractive material.

4. Summary and outlook

In this paper we compared two models for compensating unmodeled effects in the is situ transmittance measurements to improve the results of the fit algorithms used by the thickness monitoring of optical filter production. Additionally, different fitting strategies were analyzed with the result that the triangular strategy together with factor model compensation of spectra has advantages compared to the pre-calculation fit only. Therefore, using the triangular strategy also for thickness monitoring during layer deposition might further reduce the thickness errors. To investigate the feasibility of this approach, the time consumption of both strategies was determined. While the time is sufficient for coating designs with a low number of layers, the results indicate that this might not be the case for coating designs with 100 or more layers.

Therefore, a future approach would be to restrict the triangular strategy to the last *N* layers instead of all previous layers. The goal is to benefit from the advantage of fitting multiple layer thicknesses at once, while still considering the time limitations resulting from the coating setup. The value of *N* could even be automatically adapted to the computing hardware and the actual coating design.

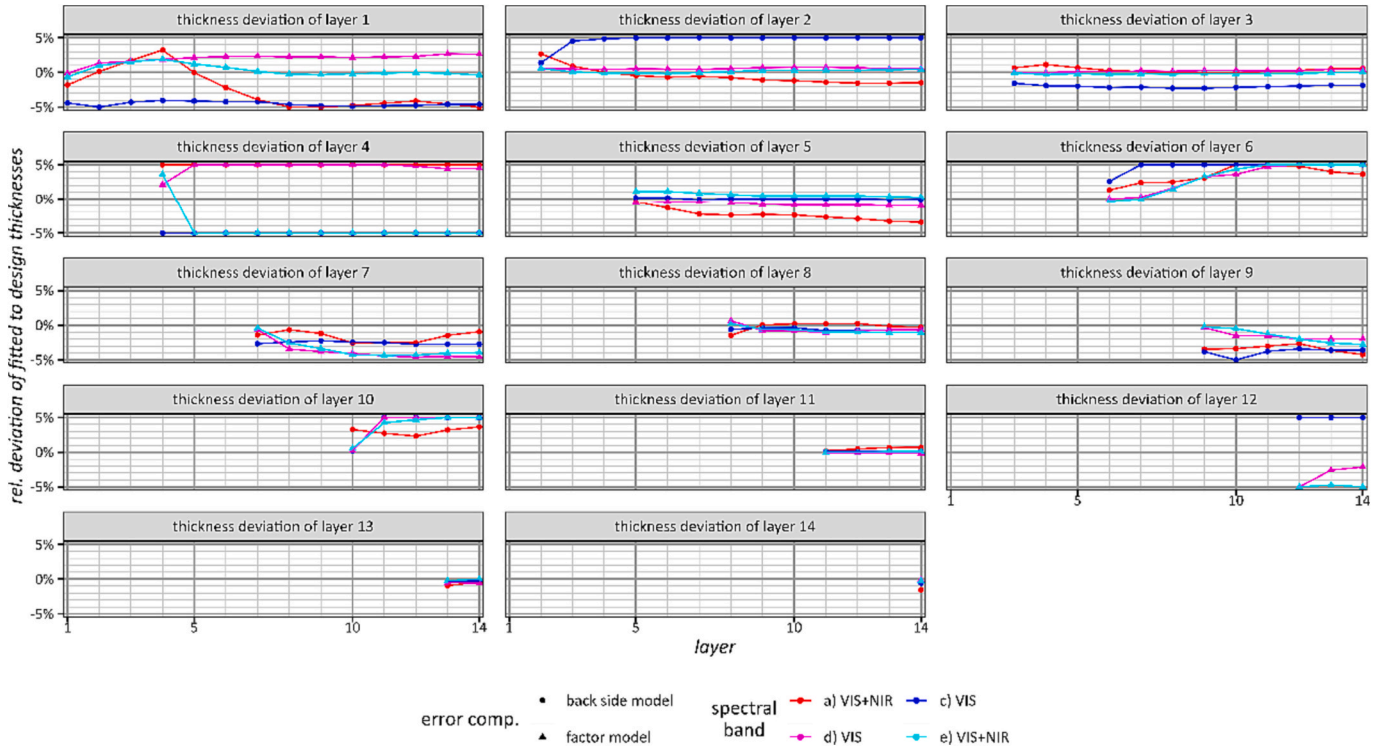

Fig. 8. Thickness fit evolution for different test conditions explained above for triangular fit shown for a 14-layer AR coating.

Funding

German Federal Ministry of Education and Research (BMBF) (13N14583).

CRediT authorship contribution statement

Thomas Melzig: Writing – original draft. **Tatiana Amochkina:** Writing – review & editing. **Stefan Bruns:** Writing – review & editing. **Philipp Farr:** Supervision. **Jörg Terhürne:** Writing – review & editing. **Michael Trubetskov:** Writing – review & editing. **Michael Vergöhl:** Supervision.

Declaration of competing interest

The authors declare the following financial interests/personal relationships which may be considered as potential competing interests:

Thomas Melzig, Stefan Bruns, Philipp Farr, Jörg Terhürne and Michael Vergöhl report financial support was provided by Federal Ministry of Education and Research Berlin Office. Thomas Melzig, Stefan Bruns, Philipp Farr, and Michael Vergöhl report a relationship with Fraunhofer Institute for Surface Engineering and Thin Films IST that includes: employment. Jörg Terhürne reports a relationship with Bte Bedampfungstechnik GmbH that includes: employment. Michael Trubetskov reports a relationship with OTF Studio GmbH that includes ownership and a relationship with Max-Planck Institute of Quantum Optics that includes: employment. Tatiana Amochkina reports a relationship with OTF Studio GmbH that includes: employment. Stefan Bruns and Michael Vergöhl have patents pending to Fraunhofer Gesellschaft.

Data availability

The data that has been used is confidential.

Acknowledgments

The work was partly funded by the German Federal Ministry of Education and Research (BMBF) within the project EPIC-Lens (FKZ 13N14583).

Portions of this work were presented at the SVC TechCon in 2023, PC5, “Extending the potential of optical monitoring software by full machine control and quality assurance”.

References

[1] A. Zoeller, M. Boos, H. Hagedorn, W. Klug, C. Schmitt, High accurate in situ optical thickness monitoring for multilayer coatings, SVC Annual Technical Conference Proceedings (2004) 72–75.

[2] D. Ristau, H. Ehlers, T. Groß, M. Lappschies, Optical broadband monitoring of conventional and ion processes, Appl. Optics 45 (7) (2006) 1495–1501.

[3] D. Ristau, H. Ehlers, S. Schlichting, M. Lappschies, State of the art in deterministic production of optical thin films, SPIE 7101 (71010C) (2008) 1–14.

[4] S. Waldner, R. Benz, P. Biedermann, A. Jaunzens, Broadband optical monitoring combined with additional rate measurement for accurate and robust coating processes, Optical Interference Coatings TuC10 (2010) 1–3.

[5] Stefan Bruns, Philipp Farr, Thomas Melzig, Jörg Terhürne, Michael Vergöhl, Improving optical thickness monitoring by including systematic and process-influenced transmittance deviations, Appl. Optics 62 (2023) B141–B147.

[6] Patent: Michael Vergöhl, Daniel Rademacher, Hans-Ulrich Kricheldorf, Günter Bräuer, “Method and device for producing low-particle layers on substrates”, EP2735018B1.

[7] M. Vergöhl, D. Rademacher, A. Pflug, Progress on optical coatings deposited with dual rotatable magnetrons in a sputter up system, Surf. Coat. Technol. 241 (2014) 38–44.

[8] Michael Vergöhl, Stefan Bruns, Daniel Rademacher, Günter Bräuer, Industrial-scale deposition of highly uniform and precise optical interference filters by the use of an improved cylindrical magnetron sputtering system, Surf. Coat. Technol. 267 (2015) 53–58.

[9] Patent: Michael A. Scobey, Richard I. Seddon, James W. Seeser, R. Russel Austin, Paul M. LeFebvre, Barry W. Manley, “Magnetron sputtering apparatus and process”, US4851095A.

[10] S. Bruns, et al., Recent developments in precision optical coatings prepared by cylindrical magnetron sputtering, Proc. SPIE 9627, Optical Systems Design: Advances in Optical Thin Films V (2015) 127–133, 96270N.

[11] S. Bruns, et al., UV bandpass filters based on Ta_2O_5 and ZrO_2 for solar observation, Proc. SPIE 11852 (2020). ICSO, 118521P.

[12] T. Groß, M. Lappschies, K. Starke, D. Ristau, Systematic errors in broadband optical monitoring, in: Optical Interference Coatings, OSA Technical Digest Series, Optica Publishing Group, 2001 paper ME4.
[13] A.V. Tikhonravov, M.K. Trubetskov, M.A. Kokarev, T.V. Amotchkina, A. Duparr, E. Quesnel, D. Ristau, S. Günster, Effect of systematic errors in spectral photometric data on the accuracy of determination of optical parameters of dielectric thin films, Appl. Optics 41 (2002) 2555–2560.
[14] A.V. Tikhonravov, M.K. Trubetskov, T.V. Amotchkina, Investigation of the effect of accumulation of thickness errors in optical coating production by broadband optical monitoring, Appl. Optics 45 (2006) 7026–7034.
[15] A.V. Tikhonravov, M.K. Trubetskov, T.V. Amotchkina, G. DeBell, V. Pervak, A. K. Sytchkova, Optical parameters of oxide films typically used in optical coating production, in: Optical Interference Coatings, OSA Technical Digest, Optica Publishing Group, 2010 (paper ThA6).